CHAPTER 3

MONOMER PREPARATION AND INSTRUMENTAL METHODS

3.1 CHEMICALS, APPARATUS AND INSTRUMENTS

3.1.1 Chemicals

The various chemicals which were used in this research project were as shown in Table 3.1 below:

Table 3.1 Chemicals used in this research project.

CHEMICAL	USAGE	GRADE	SUPPLIER
Stannous octoate	Initiator	95%	Sigma
Stannous oxalate	Initiator	Puriss	Fluka
p-Toluene sulphonic acid	Catalyst	LAB Grade	Aldrich
Antimony trioxide	Catalyst	> 98%	BDH
L(+)-Lactic acid	Monomer	90%	Fluka
Chloroform	Solvent	Commercial Grade	ICI
Methanol	Solvent	Commercial Grade	Northern
Ethyl acetate	Solvent	Commercial Grade	Northern

Table 3.1 (Continued)

CHEMICAL	USAGE	GRADE	SUPPLIER
Sodium sulfate (anhydrous)	Drying agent	AR Grade	Merck
Molecular sieves type 4 Å	Drying agent	Standard	Fluka
Calcium chloride	Drying agent	LAB Grade	BDH

3.1.2 Apparatus and Instuments

The main items of apparatus and instruments used were as given in Table 3.2.

Table 3.2 Apparatus and instruments used in this research project.

APPARATUS AND INSTRUMENTS	COMPANY	MODEL
FT-IR Spectrometer	Nicolet	510
60 MHz ^{1}H-NMR Spectrometer	Hitachi	R-1500
Differential Scanning Calorimeter	Perkin-Elmer	DSC 7
Automatic Viscosity Measuring System	Schott-Gerate	AVS 300
Controlled Atmosphere Glove Box	Labconco	50004
Vacuum Oven	Eyela	VOS–300SD
Rotary Evaporator	Buchi	B-480

3.2 INSTRUMENTAL METHODS

3.2.1 Infrared Spectroscopy (IR) [17, 22]

Infrared spectroscopy is probably the most extensively used method for the investigation of polymer structure and the analysis of functional groups. IR spectrometers have been used to study samples in the gaseous, liquid, and solid state, depending on the types of accessories used. IR has been used to characterize polymer blends, dynamics, surfaces, and interfaces, as well as chromatographic effluents and degradation products. It is capable of qualitative identification of the structure of unknown materials as well as the quantitative measurement of the components in a complex mixture. There are compilations of infrared spectra including indices to collections of spectra and to the literature.

Infrared radiation is absorbed when the oscillating dipole moment caused by a molecular vibration interacts with the oscillating electric vector of the infrared beam. A complex molecule has a large number of vibrational modes. Some of these molecular vibrations are associated with the vibrations of individual bonds or functional groups (localized vibrations) while others must be considered as vibrations of the whole molecule.

Infrared spectroscopy is a relatively simple technique, non-destructive, and versatile enough to analyze solids, liquids, and gases with a minimum of sample preparation. Polymers can be mixed with potassium bromide and then pressed into pellets. Films can be prepared from melts or cast from solution and can be studied easily. In bulk samples or powders, or if a concentration profile is needed, the reflectance technique is probably more suitable than transmission.

Most recently, Fourier-transform IR spectroscopy (FT-IR) has proved to be a powerful tool in polymer characterization. However, it has been applied only to the observation of events that are stationary in time, or at least stationary with respect to the measurement time. The multiplex characteristics (the ability to measure all spectral elements) of the interferometer, together with the high energy throughput, provide FT-IR with a substantial gain in signal-to-noise ratio for a given measurement time, as compared to a normal dispersive IR instruments. Hence, the use of FT-IR to study time-dependent phenomena is feasible, the advantage being that simultaneous measurements of band position, shape and relative intensity are made.

Despite the great improvement in the measurement timescale when FT-IR is used, it is impractical, if not impossible, for the interferometer to follow rapidly evolving events with time resolution of the order of milliseconds. The limit is reached when the time period required for one scan of the moving mirror is longer than the time resolution required to describe the physical phenomena. Furthermore, in order to improve the signal-to-noise ratio, co-adding scans are necessary, a procedure which further degrades the time resolution. Therefore, a number of time-resolved FT-IR techniques have recently been developed to increase the speed of data acquisition to a value suitable for characterizing the dynamics of structural changes in polymers.

In this research project, a Nicolet Model FT-IR 510 Infrared Spectrometer was used for the recording of all monomer and polymer infrared spectra.

3.2.2 High-Resolution Nuclear Magnetic Resonance Spectroscopy (^{1}H-NMR) [17, 22-23]

Nuclear magnetic resonance (NMR) spectroscopy is a most effective and significant method for observing the structure and dynamics of polymer chains both in solution and in the solid state. Undoubtedly the widest application of NMR spectroscopy is in the field of structure determination. The identification of certain atoms or groups in a molecule as well as their position relative to each other can be obtained by one-, two-, and three-dimensional NMR. Of importance in the polymerization of vinyl monomers is the orientation of each vinyl monomer unit to the growing chain tacticity. The timescale involved in NMR measurements makes it possible to study certain rate processes, including chemical reaction rates. Other applications are isomerism, internal relaxation, conformational analysis, and tautomerism.

The frequency of the energy required to induce spin-state flipping of nuclei varies directly with the magnitude of the applied magnetic field. The larger the field, the larger the difference between parallel and antiparallel spin states and the higher the energy of the signal required to induce the change. Commercial spectrometers have very large magnets that employ superconducting wires to produce the magnetic field. With these field strengths, electromagnetic energy in the radiofrequency range is required. Spectrometers are classified by the frequency used to change the spin state of magnetically active nuclei. The highest-field machines currently available from commercial instrument manufacturers operate at 750 MHz, although instruments using from 100 to 300 MHz signals are much more common. However, for simple organic compounds, 60 MHz is usually sufficient for routine analysis.

In this research project, the particular instrument used for structural characterization was a Hitachi 60 MHz Model R-1500 ^{1}H-NMR Spectrometer.

3.2.3 Differential Scanning Calorimetry (DSC) [17, 22, 24]

Differential scanning calorimetry (DSC) is a thermoanalytical technique in which the difference in energy input into a substance and a thermally inert reference is measured as a function of temperature while the substance and reference material are subjected to a controlled temperature program. The sample is submitted to linear heating and the rate of heat flow in the sample, proportional to the instantaneous specific heat, is measured continuously. Inside the measuring cell, which is normally kept at room temperature, two symmetrical pans are fixed. The platinum resistance thermometer and the heating unit built into the sample holders serve as a primary temperature control of the system. The secondary temperature control system maintains the temperature difference between the two holders at zero by means of a heating current which is measured. In other words, the temperature of the sample is kept the same as that of the reference sample (or the block) by introducing heat into the reference sample. This amount of heat is recorded as a function of time or temperature.

A number of important physical changes in a polymer may be measured by DSC. These include the glass transition temperature (T_g), the crystallization temperature (T_c), the melt temperature (T_m), and the degradation or decomposition temperature (T_d). The DSC method can also be applied to the direct measurement of the energy absorbed or evolved in studies of heats of fusion, heats of reaction (including polymerization, crosslinking, oxidation and combustion), and specific heats. The usual temperature range covered is –150 to 725 $^{\circ}$C. Greatest accuracy in temperature measurement is attained by observing the following four considerations:

1). Precise calibration of the instrument

2). Small sample size ($\leq$ 5 mg)

3). Proper encapsulation of the sample

4). Slow scanning rate ($\leq$ 10°C/min)

For precise measurement of heats of transition, it is necessary to add two further considerations:

1). Precise weighing (± 0.01 mg)

2). Precise calculation of the peak area lying under the endotherm or exotherm caused by the transition

From the DSC curve, the area under a transition peak is directly proportional to the energy of the change per unit weight.

In this research project, the instrument used was a Perkin-Elmer DSC7 Differential Scanning Calorimeter operating from 20 °C upwards.

3.2.4 Dilute-Solution Viscometry [17, 22, 24-25]

Dilute-solution viscometry is principally based on the fact that the viscosity of a polymer solution is higher than that of the pure solvent. The large difference in size between solute and solvent molecules gives rise to this effect. The change in viscosity can be significant even at low polymer concentrations, especially for polyelectrolytes and polymers with high molecular weights. Dilute-solution viscometry is concerned with accurate quantitative measurement of the increase in viscosity and allows determination of the intrinsic ability of a polymer to increase the viscosity of a particular solvent at a given temperature. This quantity provides information relating to the size of the polymer in solution, including the effects on chain dimensions of polymer structure, molecular shape, degree of polymerization, and polymer-solvent interaction. Most commonly, however, dilute-solution viscometry is used to estimate the molecular weight of a polymer, which involves the use of semi-empirical equations that have to be established for each polymer-solvent-temperature system by analysis of polymer samples whose

molecular weights are known. The advantage of dilute-solution viscometry is that it is simple, fast, and inexpensive. It is applicable over the complete range of attainable molecular weights. The disadvantage is that it provides estimates of molecular weight that are not absolute.

3.2.4.1 Definitions of Dilute-Solution Viscometry

In dilute-solution viscometry, a variety of quantities are to be found in the literature describing the experimental data. There are summarized in Table 3.3.

Table 3.3 Nomenclature and definitions used in dilute-solution viscometry.

COMMON NAME	IUPAC NAME	SYMBOL AND DEFINING EQUATION
Viscosity	Viscosity coefficient	η
Relative viscosity	Viscosity ratio	$\eta_{rel} = \eta/\eta_o \approx t/t_o$
Specific viscosity	-	$\eta_{sp} = \eta_{rel} - 1 = (\eta - \eta_o) \approx (t - t_o)/t_o$
Viscosity number	Reduced viscosity	$\eta_{red} = \eta_{sp}/c$
Inherent viscosity	Logarithmic viscosity	$\eta_{inh} = (\ln\eta_{rel})/c$
Intrinsic viscosity	Limiting viscosity number	$[\eta] = (\eta_{sp}/c)_{c\rightarrow 0} = [(\ln\eta_{rel})/c]_{c\rightarrow 0}$

The relative viscosity, η_{rel}, may be written very simply as a ratio of the viscometer flow–times if the density and kinetic energy corrections are neglected:

$$\eta_{rel} = \frac{\eta}{\eta_o} = \frac{t}{t_o} \qquad .....(3.1)$$

where t and t_o are the flow–times of the polymer solution and solvent respectively. Obviously, η and η_o (i.e. t and t_o) must be measured under the same conditions. The relative viscosity is always greater than unity because the presence of the polymeric solute always increases the viscosity of the solvent. It is appropriate then to define the **specific viscosity**, η_{sp}, as the fractional increase in viscosity caused by the presence of the dissolved polymer in the solvent, as shown in equation 3.2.

$$\eta_{sp} = \frac{\eta - \eta_o}{\eta_o} = \eta_{rel} - 1 \qquad \text{....(3.2)}$$

The specific viscosity and the relative viscosity clearly depend on the concentration, c, of the polymer in solution; in fact, they increase in magnitude with increasing concentration. Therefore, η_{sp} can be expressed as a reduced quantity called the **reduced viscosity**, η_{red}.

$$\eta_{red} = \frac{\eta_{sp}}{c} \qquad \text{.....(3.3)}$$

where **c** is usually expressed in units of g dl^{-1} (g/100ml).

A similar relationship exists for the **inherent viscosity**, η_{inh}, as given by:

$$\eta_{inh} = \frac{\ln \eta_{rel}}{c} \qquad \text{.....(3.4)}$$

Finally, the intrinsic viscosity, $[\eta]$, is defined as the limits of both the reduced viscosity and the inherent viscosity as the concentration approaches zero, and is therefore given by:

$$[\eta] = (\eta_{sp} / c)_{c \rightarrow 0} = [(\ln \eta_{rel}) / c]_{c \rightarrow 0} \quad \text{..... (3.5)}$$

3.2.4.2 Calculation of Intrinsic Viscosity

The intrinsic viscosity term, $[\eta]$, is the term which is directly related to the polymer's average molecular weight and is most commonly and conveniently determined via the Huggins Equation

$$\eta_{red} = \eta_{sp} / c = [\eta] + k' [\eta]^2 c \quad \text{..... (3.6)}$$

and the Kraemer Equation

$$\eta_{inh} = (\ln \eta_{rel}) / c = [\eta] + k'' [\eta]^2 c \quad \text{..... (3.7)}$$

In these Huggins and Kraemer Equations, c is the concentration of the polymer in units of g dl^{-1}, $[\eta]$ therefore has units of dl g^{-1}, k' is the Huggins constant which usually has a value in the range $0.3 < k' < 0.5$, and k" is the Kraemer constant which is usually negative. Furthermore, both k' and k" are interaction constants for a given polymer in a given solvent at a given temperature and are themselves related by the equation:

$$k' - k'' = 0.5 \quad \text{..... (3.8)}$$

Thus, in accordance with the forms of equations (3.6) and (3.7), from the linearity of the plots of η_{red} and η_{inh} versus c, $[\eta]$ may be obtained by extrapolating each plot to c = 0, as shown in Figure 3.1. The double extrapolation to a common point facilitates the accurate estimation of $[\eta]$.

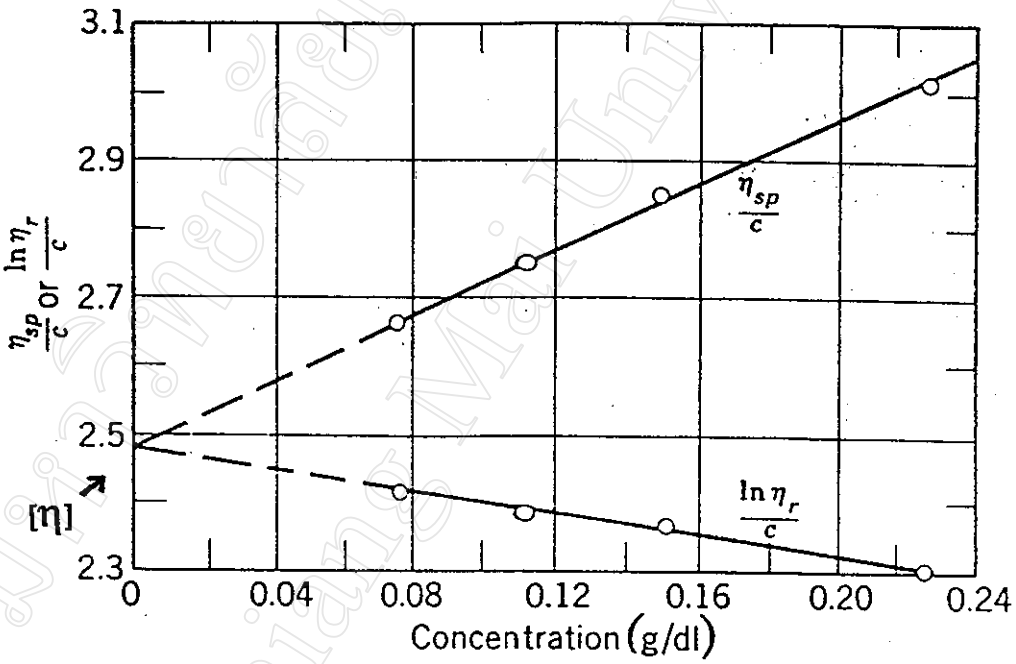

Figure 3.1 Reduced and inherent viscosity–concentration curves for a typical polymer sample [25].

3.2.4.3 Intrinsic Viscosity – Molecular Weight Relationship

The intrinsic viscosity, $[\eta]$, of a polymer in solution is related to its molecular weight by the Mark – Houwink – Sakurada Equation:

$$[\eta] = K \bar{M}_V^a \quad \text{..... (3.9)}$$

where:

$\bar{M}_V$ is the so-called "viscosity-average molecular weight" and K and a are constants for a given polymer – solvent – temperature system. The value of a, which increases with the solvent power of the medium, is usually between 0.5 and 0.8 in polymer solutions. K generally has values in the range of 10^{-4} to 10^{-6} dl/g and tends to decrease as a increases. A comprehensive collection of K and a values are to be found in the **Polymer Handbook** [26].

Estimates of the level of molecular weight based on intrinsic viscosity are roughly as follows:

Low $\bar{M}v$	$(< 10^4)$	: $[\eta]$ less than 0.2 dl/g
Medium $\bar{M}v$	$(\approx 10^4 - 10^5)$	: $[\eta]$ greater than 0.2 dl/g but less than 0.8 dl/g
High $\bar{M}v$	$(> 10^5)$	: $[\eta]$ greater than 0.8 dl/g

3.2.5 Gravimetry [17]

The most direct way of obtaining conversion data for polymerization is by gravimetric determination of the polymer formed. The most obvious and straightforward way to do this is to stop the reaction at some predetermined time (e.g., by a sudden chilling of the reaction mixture) and then separate the monomer reactant from the polymeric product. The amount of monomer remaining or the amount of polymer formed

at this reaction time is then determined by weighing. This process can then be repeated for other reaction times until sufficient information has been obtained.

However, this gravimetric method is time–consuming and requires the preparation of a new reaction mixture for each experimental point on the conversion–time plot. Moreover, this technique has been criticized as being too laborious, extremely clumsy and susceptible to several errors, e.g., inclusion of monomer and/or solvent with the precipitated polymer, loss of low molecular weight material, uncontrolled polymerization conditions for the different reaction tubes within one series, etc. On the other hand, this method is useful as a standard method since absolute conversions are obtained from it.

The % conversion is simply calculated from:

$$\% \text{ conversion} = \frac{\text{weight of polymer obtained}}{\text{initial weight of monomer}} \times 100 \quad .....(3.10)$$

The equation assumes, of course, no loss of weight due to any by-product formation, as was the case in the ring-opening polymerizations studied here. The above-mentioned errors were minimized as far as possible by:

(a) Polymerizing each series of samples simultaneously in the same heating bath

(b) Choosing a suitable solvent / non–solvent combination which allowed the polymer to precipitate in as fine a particle size as possible, amenable to efficient drying

(c) Allowing the polymer to precipitate as completely as possible by prolonged stirring and then standing in an ice–bath before filtering and washing

(d) Assiduous drying to constant weight in a vacuum oven at an appropriate temperature

3.3 L-LACTIDE PREPARATION, PURIFICATION AND STRUCTURAL ANALYSIS

The monomer used in this research project was L(-)-lactide. Since L(-)-lactide is prohibitively expensive to buy, it was synthesized from its much cheaper precursor, L(+) – lactic acid. The method of synthesis is described below.

3.3.1 Method of Synthesis

In a typical synthesis reaction in this research project, approximately 200 g of L (+)-lactic acid together with approximately 2.00 g of p-toluenesulphonic acid catalyst (1% by weight) were heated at 160 °C under a nitrogen atmosphere in a conventional short – path distillation apparatus (Figure 3.2a). Heating was continued for about 5 hours until the water of polycondensation ceased to distill from the flask. The apparatus was then adapted for vacuum take–off (Figure 3.2b) and heating continued for a further 2-3 hours at a reduced pressure to facilitate further removal of water and to increase the yield of low molecular weight poly(L-lactic acid), PLLA.

Finally, for an additional period of about 4 hours, 1% by weight of antimony trioxide degradation catalyst was added and the heating temperature increased up to 220 – 240 °C under a reduced pressure of 4-5 mm Hg in order to thermally degrade the low molecular weight PLLA to yield L(-)-lactide as the primary product. Crude L(-)-lactide began to distill out of the flask and solidify in the air condenser as light brown, needle-like crystals. This crude product was obtained in approximately 70–80% yield based on the initial amount of L(+)-lactic acid.

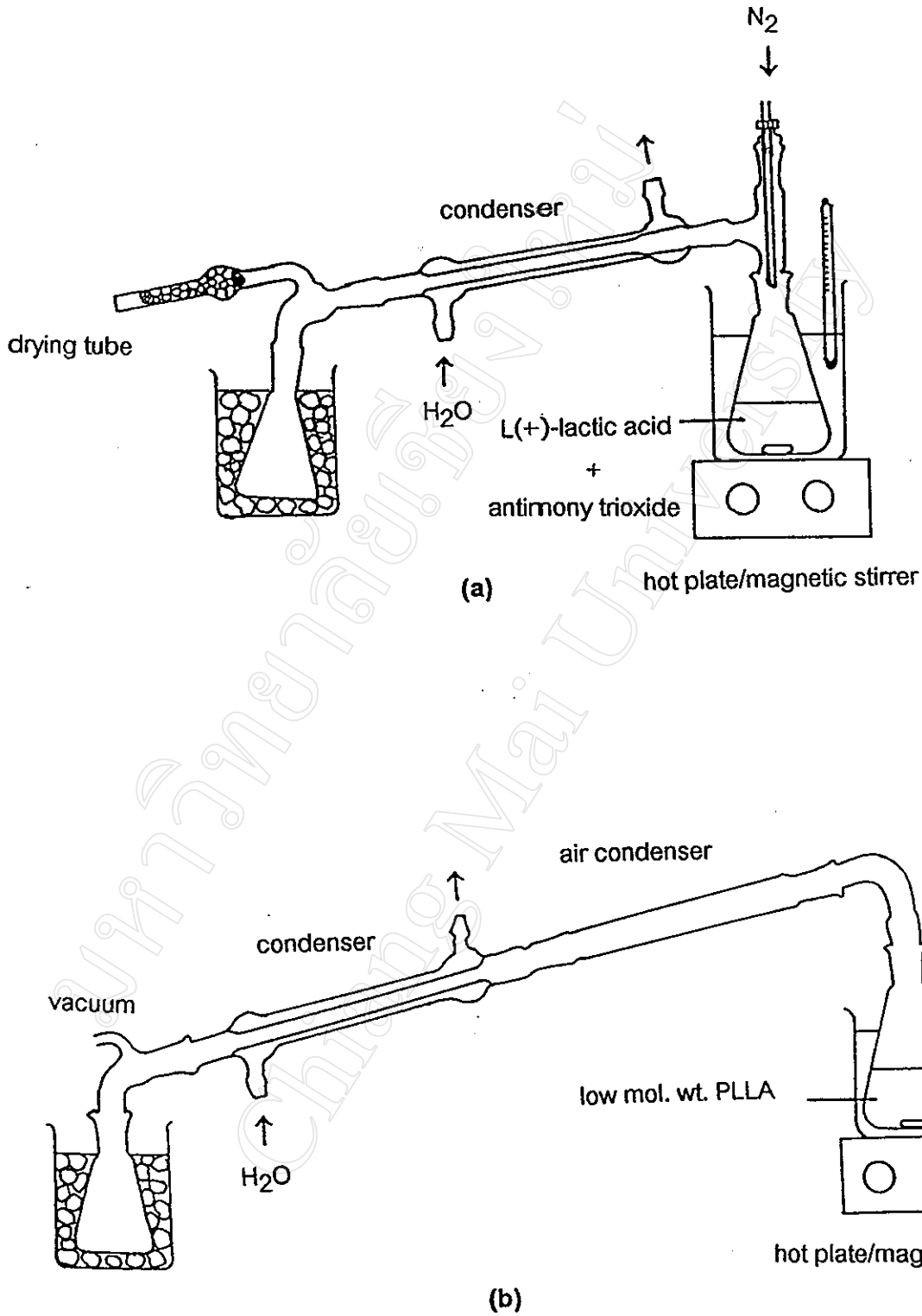

Figure 3.2 Apparatus used in the two-step synthesis of L-lactide:

(a) L(+)-lactic acid polycondensation to low mol. wt. PLLA

(b) thermal decomposition of low mol. wt. PLLA to L(-)-lactide

3.3.2 Purification and Purity Analysis

The crude L-lactide was carefully and quickly removed from the air condenser due to its hygroscopic nature. It was then purified by recrystallization three times from distilled ethyl acetate to yielded pure L-lactide as a white, needle–like, crystalline solid. It was dried to constant weight in a vacuum oven at 50 °C and stored in a vacuum desiccator over silica gel. The final purified product was obtained in approximately 60–70% yield. Analysis by differential scanning calorimetry (DSC) showed that the purified L-lactide had a DSC melting peak from 95 to 97 °C (Figure 3.3).

In order to determine the actual purity of the recrystallized L-lactide by the DSC technique, the instrument's Purity Analysis Software Program was employed [27]. To obtain the best results from purity analysis, a slow heating rate (2 °C /min or less) and a small sample size in the range of 1-3 mg are recommended. From its DSC melting curve (Figure 3.3), a purity of 99.77% was obtained. This was considered satisfactory for polymerization purposes from the point of view of obtaining high molecular weight poly(L-lactide). The underlying thermodynamic theory of this purity analysis method is given in an Appendix at the end of this thesis.

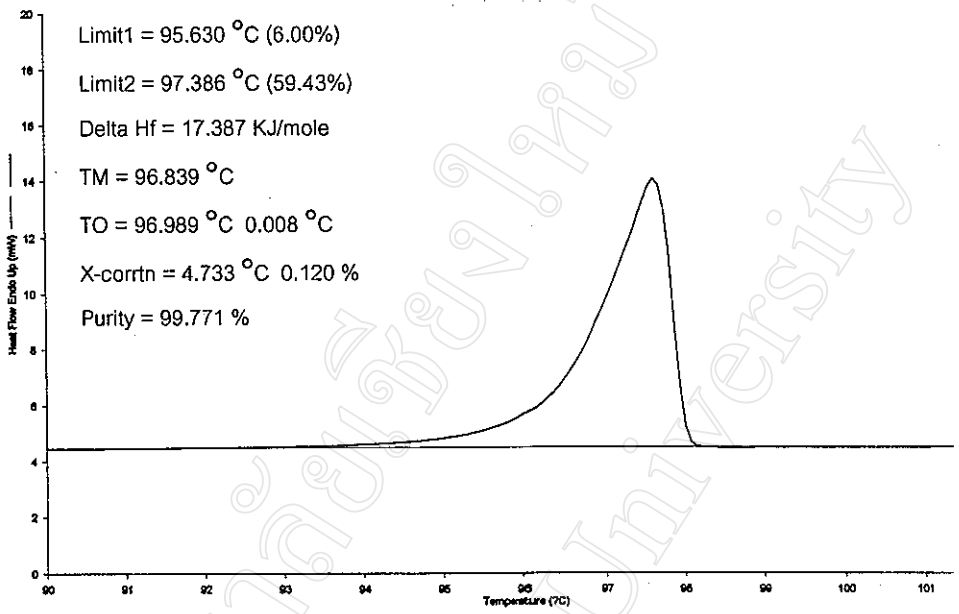

Figure 3.3 DSC melting curve of synthesized L-lactide (after 3rd recrystallization). (Sample size = 2.820 mg, heating rate = 2 °C/min)

3.3.3 Structural Analysis by IR and ^{1}H-NMR Spectroscopy

The IR spectra of the L(+)-lactic acid that was used in this work and the purified L(-)-lactide are shown in Figures 3.4 and 3.6 and can be compared with the reference spectra in Figures 3.5 and 3.7 respectively. The major vibrational peaks are listed in Table 3.4.

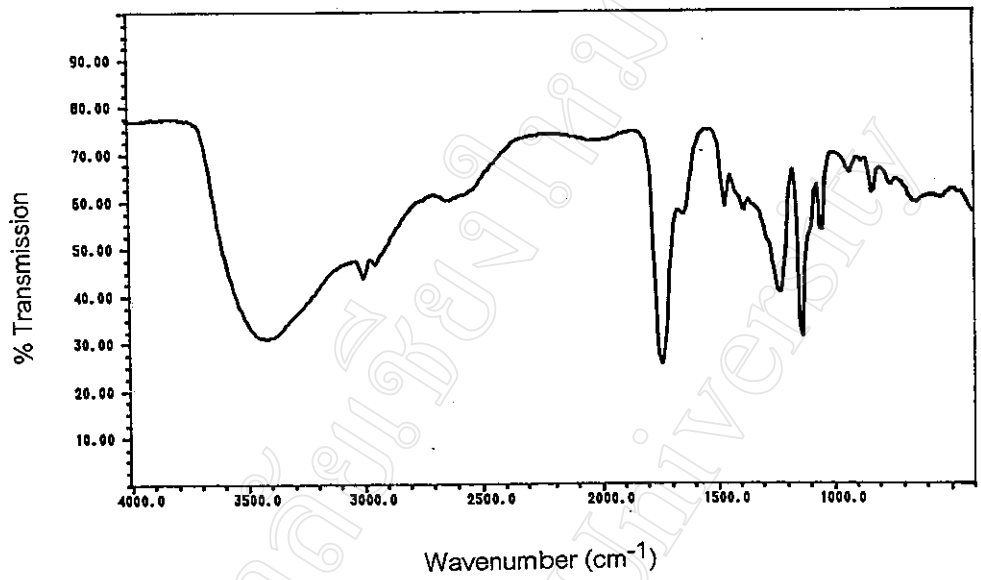

Figure 3.4 IR spectrum of the L(+)-lactic acid used in this work.

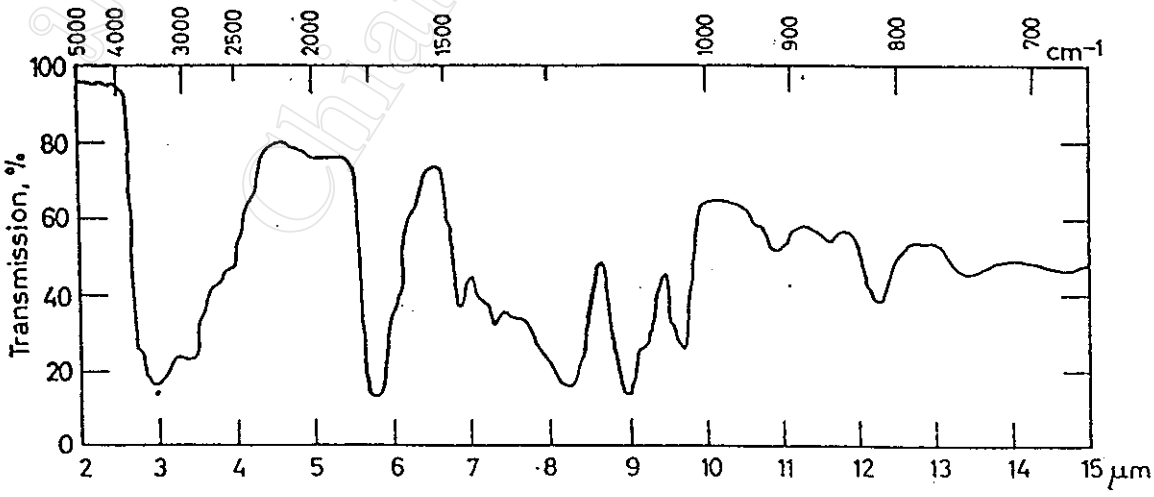

Figure 3.5 Reference IR spectrum of L-lactic acid [12].

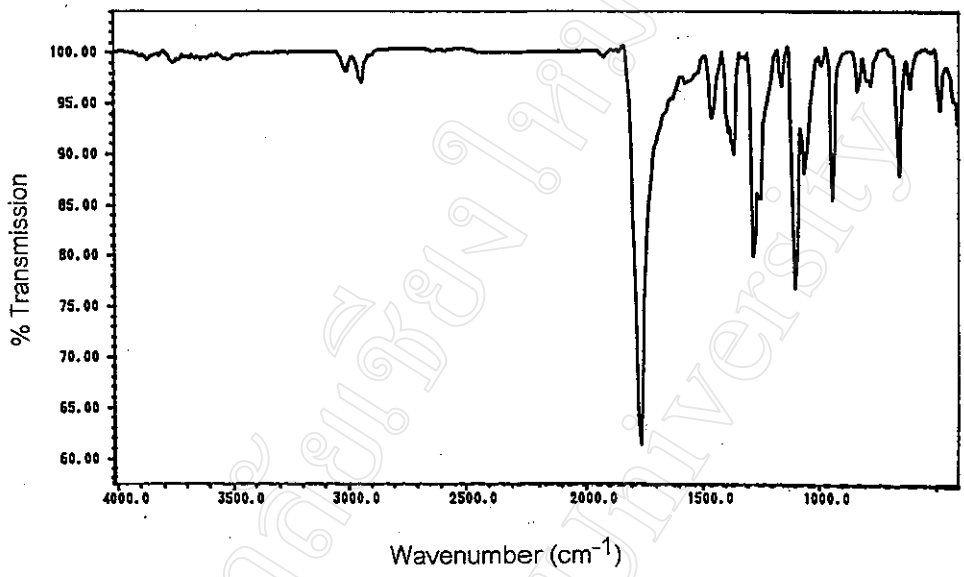

Figure 3.6 IR spectrum of the purified L(-)-lactide synthesized in this work.

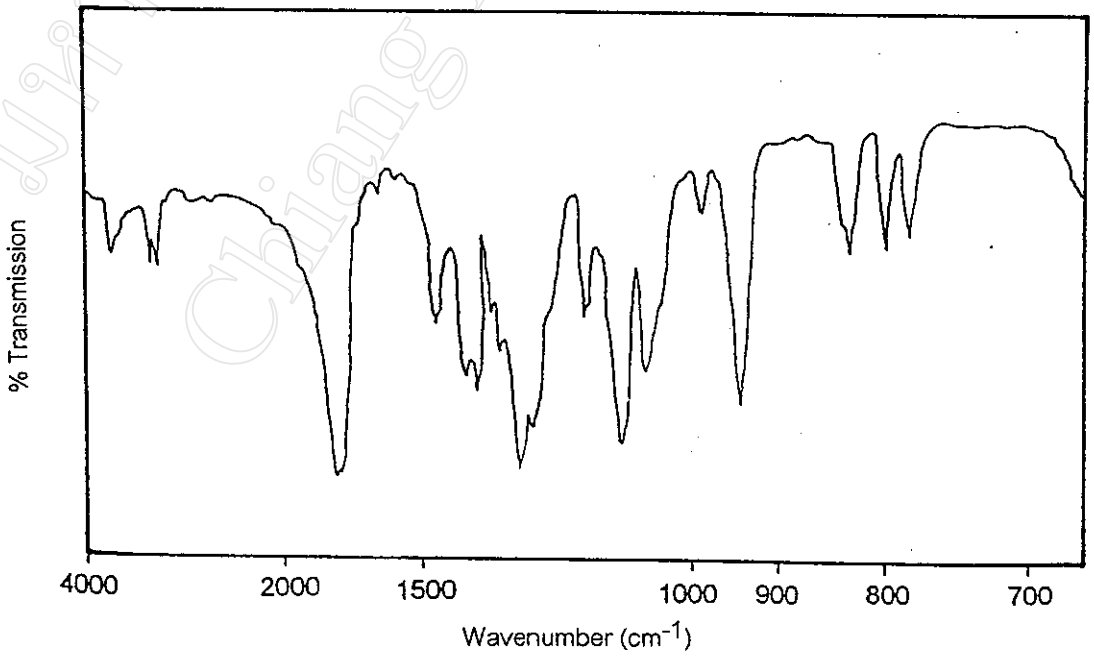

Figure 3.7 Reference IR spectrum of L-lactide [28].

Table 3.4 Main vibrational assignments in the L(+)-lactic acid and L(-)-lactide infrared spectra.

VIBRATIONAL ASSIGNMENT	WAVENUMBER (cm^{-1})	
	L(+)-lactic acid	L(-)-lactide
O – H stretching	3600 – 3000	(weak)
C – H stretching	3000 – 2600	3100 – 2900
C = O stretching	1780 – 1700	1800 – 1740
C – H bending	1460, 1380	1460, 1380
C – O stretching in acyl–oxygen	1260 – 1200	1280 – 1240 (a)
C – O stretching in alkyl oxygen	-	1100 – 1080 (b)

(a)

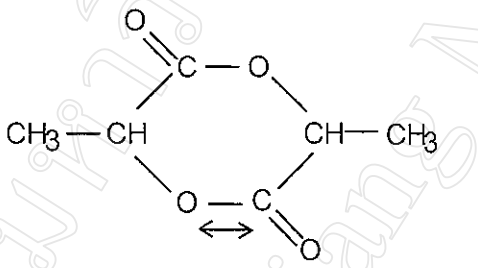

acyl - oxygen bond

(b)

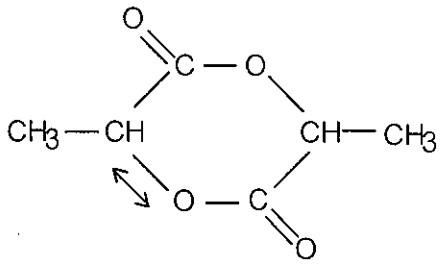

alkyl - oxygen bond

The ^{1}H-NMR spectrum of the L(+)-lactic acid that was used in this work is shown in Figure 3.8 and can be compared with the reference spectrum in Figure 3.9. The ^{1}H-NMR spectrum of the purified L(-)-lactide is shown in Figure 3.10. Both spectra were obtained from sample solutions in deuterated chloroform, $CDCl_3$, as solvent. The chemical shifts of the various peaks in the spectra are listed in Table 3.5 and the peaks assigned to the corresponding protons.

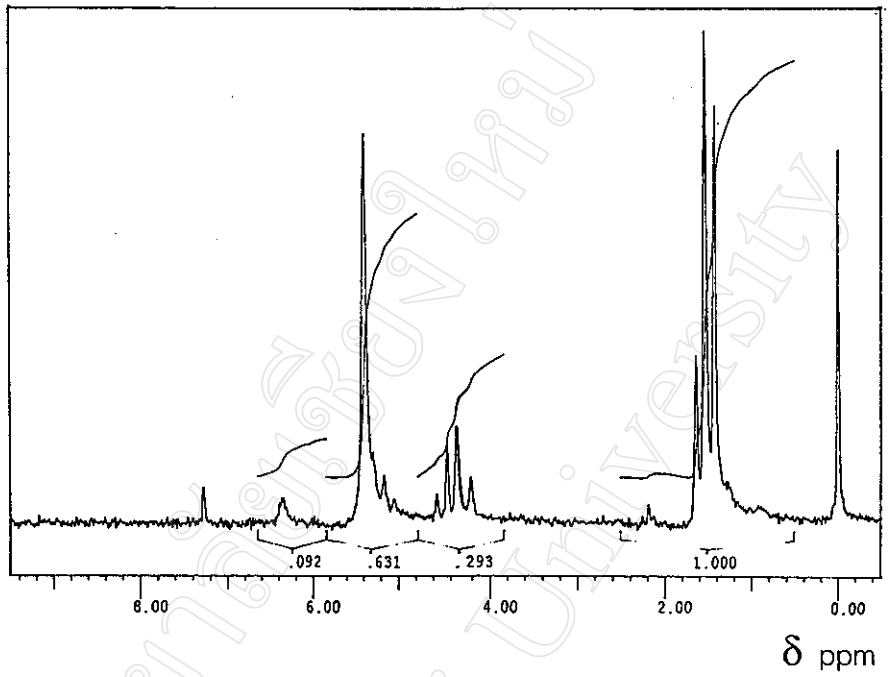

Figure 3.8 60 MHz ^{1}H-NMR spectrum of L(+)-lactic acid in $CDCl_3$ as solvent.

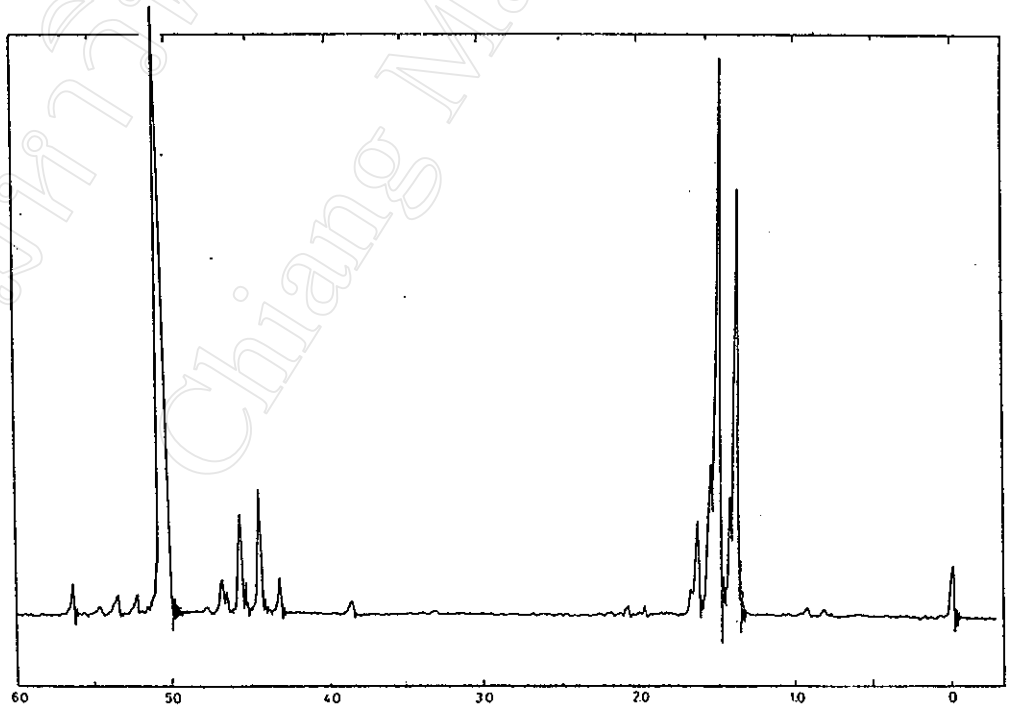

Figure 3.9 Reference ^{1}H-NMR spectrum of approximately 90% lactic acid [12].

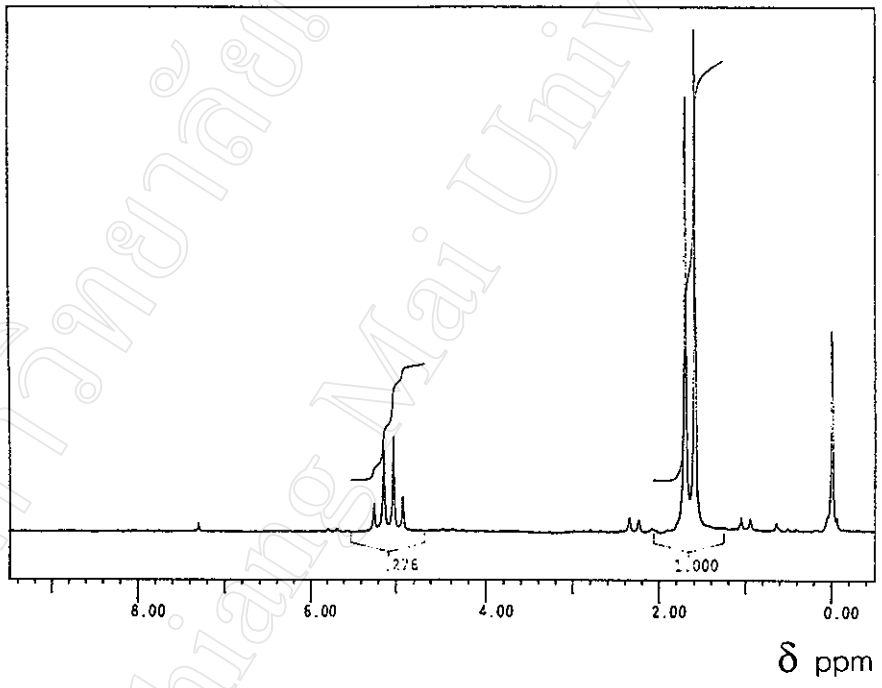

Figure 3.10 60 MHz ^{1}H-NMR spectrum of purified L(-)-lactide in $CDCl_3$ as solvent.

Table 3.5 ^{1}H-NMR chemical shifts and proton assignments for L(+)-lactic acid and L(-)-lactide.

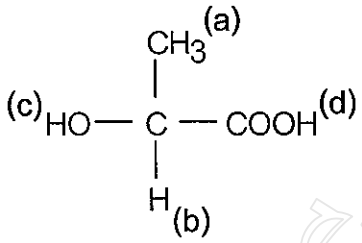

L-lactic acid

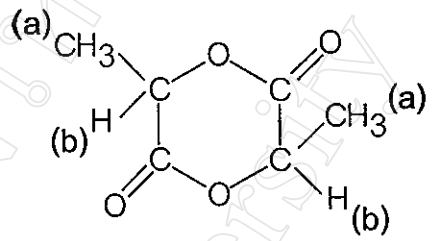

L-lactide

Proton Assignment	Chemical Shift, δ (ppm) *	
	L(+)-Lactic Acid	L(-)-Lactide
a	1.54	1.54
b	4.38	5.42
c	5.38	-
d	>10 (undetected)	-

* values taken as the approximate band centre of each multiplet

3.4 CATALYST/INITIATOR PURIFICATION

Because trace amounts of moisture and other impurities could be present in the catalysts and initiators used in this research project, they required further purification since moisture (especially) can have a serious effect on the polymer molecular weight obtained.

3.4.1 Stannous Octoate

3.4.1.1 Purification by Fractional Distillation

Commercial $Sn(Oct)_2$, typically only 95% pure as supplied, commonly contains 2-ethyl hexanoic (octanoic) acid and water as impurities, as mentioned in the previous Chapter. The acid is known to be very difficult to remove, even by careful fractional distillation under vacuum. The commercial $Sn(Oct)_2$ used in this work had a boiling point range of 102 – 104 °C / 5 – 6 mm Hg (cf. 2-ethyl hexanoic acid lit. [29] b. pt. = 140.0 °C / 23 mm Hg; $Sn(Oct)_2$ lit. b. pt. could not be found).

3.4.1.2 Structural Analysis by IR Spectroscopy

The IR spectra of the commercial and distilled $Sn(Oct)_2$ are compared in Figures 3.11 and 3.12. The spectra were obtained from neat liquid samples.

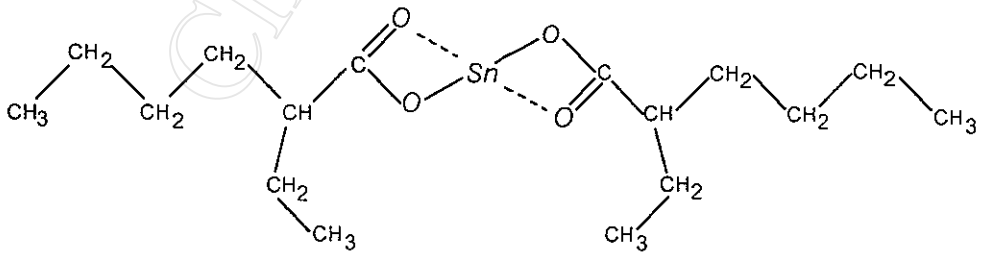

stannous octoate, $Sn(Oct)_2$

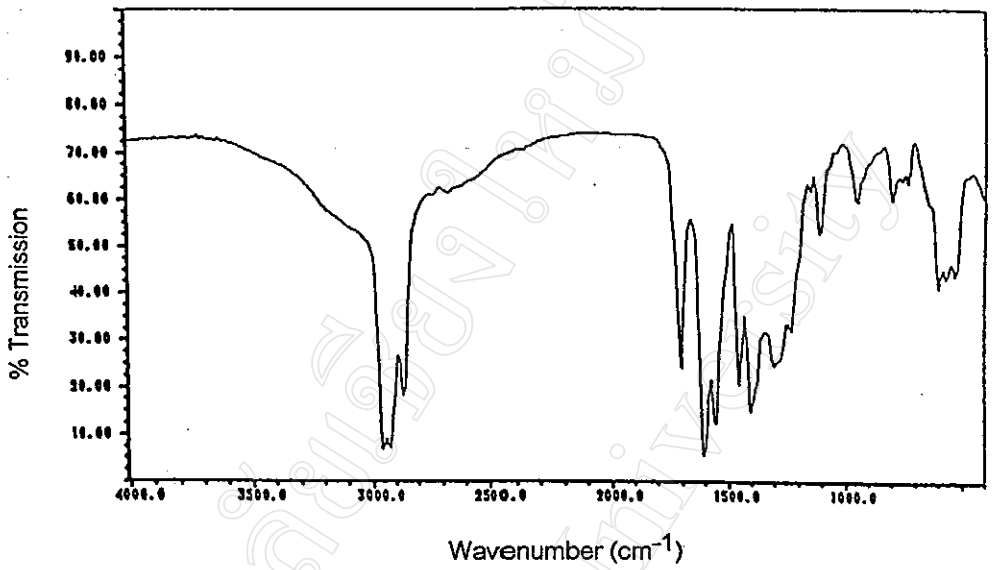

Figure 3.11 IR spectrum of commercial $Sn(Oct)_2$ before fractional distillation under vacuum.

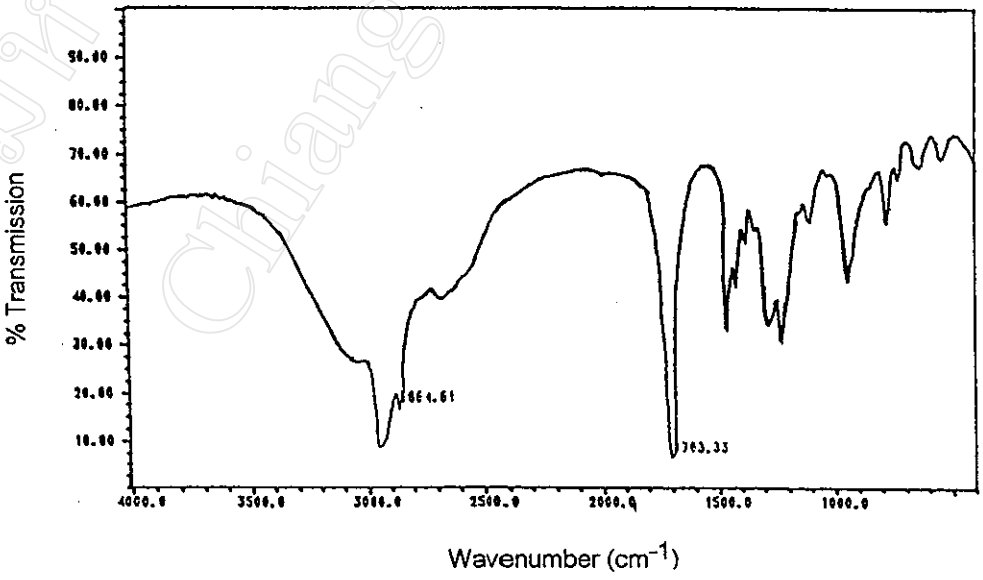

Figure 3.12 IR spectrum of distilled $Sn(Oct)_2$ after fractional distillation under vacuum.

Table 3.6 Main vibrational assignments in the commercial and distilled $Sn(Oct)_2$ infrared spectra.

VIBRATIONAL ASSIGNMENT	WAVENUMBER (cm^{-1})	
	Commercial	Distilled
O – H stretching in COOH**	3700 – 3100	3700 – 3100
C – H stretching	2950 - 2850	2950 – 2850
C = O stretching	1700	1700
Unassigned peaks*	1600, 1500	-
C – H bending	1460, 1400	1480, 1420
C – O stretching (acyl-oxygen)	1300	1290
C – O stretching (alkyl-oxygen)	1230	1230

* present only in the commercial sample

** COOH in octanoic acid impurity

On comparing the IR spectra, it appears that the free octanoic acid content, as indicated by the intensity of the carboxylic O–H stretching peak from 3700 – 3100 cm^{-1}, is actually greater in the distilled sample than in the commercial sample. A possible explanation for this could be that the $Sn(Oct)_2$ is thermally unstable at the distillation temperature (>100 ^{o}C) and partially decomposes to octanoic acid. If so, then there is clearly no advantage to be gained from distillation and it is better just to dry the commercial sample by stirring with and storage over conventional drying agents.

Consequently, in this work, the commercial $Sn(Oct)_2$ was first stirred with anhydrous sodium sulphate (coarse drying agent) before being stored over molecular sieves 4 Å (sensitive drying agent) in a tightly sealed container. Even though this did

not remove the octanoic acid impurity, it would have at least removed most if not all of the moisture which would otherwise have had an effect on the polymerization reaction. It has been reported that moisture, in conjunction with $Sn(Oct)_2$, can act as an initiator in this type of polymerization reaction [29]. Moisture can also hydrolyse $Sn(Oct)_2$ to less active Sn(II) derivatives, as described previously on page 21.

3.4.1.3 Compositional Analysis by Gas Chromatography-Mass Spectrometry (GC-MS)

The GC chromatograms of the commercial and distilled $Sn(Oct)_2$ samples are compared in Figure 3.13 and 3.14. Clearly there are differences between the two which reinforces the view that some changes in chemical composition occurred during distillation. When the compositions of individual components are compared in Figures 3.15 – 3.17, the MS spectra show some similarities to the reference spectrum of 2-ethyl hexanoic (octanoic) acid, as would be expected. (A reference spectrum of $Sn(Oct)_2$ was unfortunately not available.) The top mass peak of 405, corresponding to the molecular weight of $Sn(Oct)_2$, was only detectable in component peaks at longer retention times (e.g., in Figure 3.16). Again it is possible that, due to the high temperature (250 ^{o}C) used in the GC-MS analysis, some thermal decomposition of the sample could have occurred which complicates the interpretation of the results.

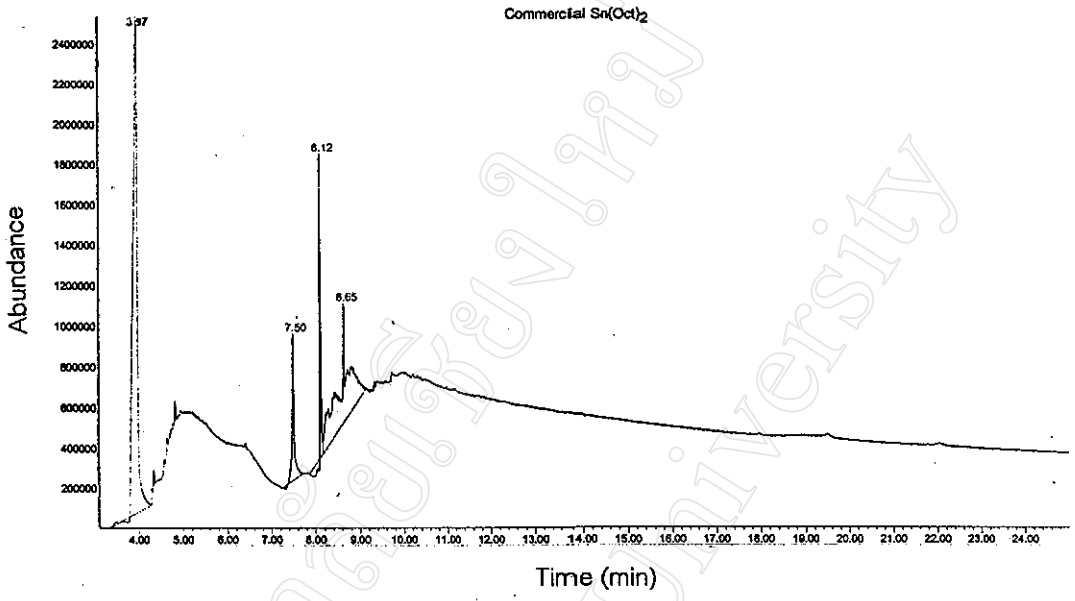

Figure 3.13 GC chromatogram of commercial $Sn(Oct)_2$.

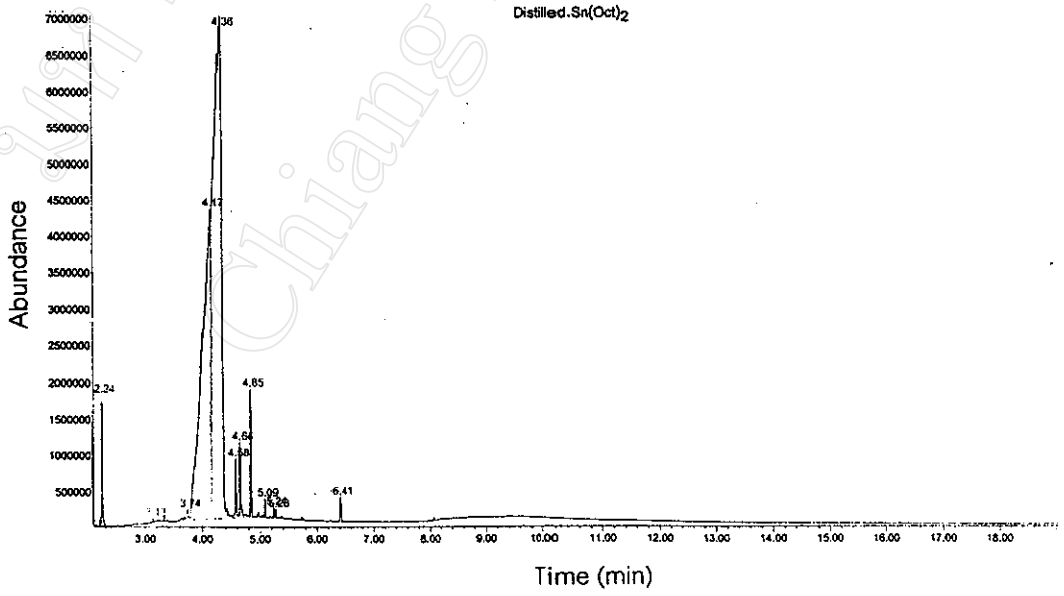

Figure 3.14 GC chromatogram of distilled $Sn(Oct)_2$.

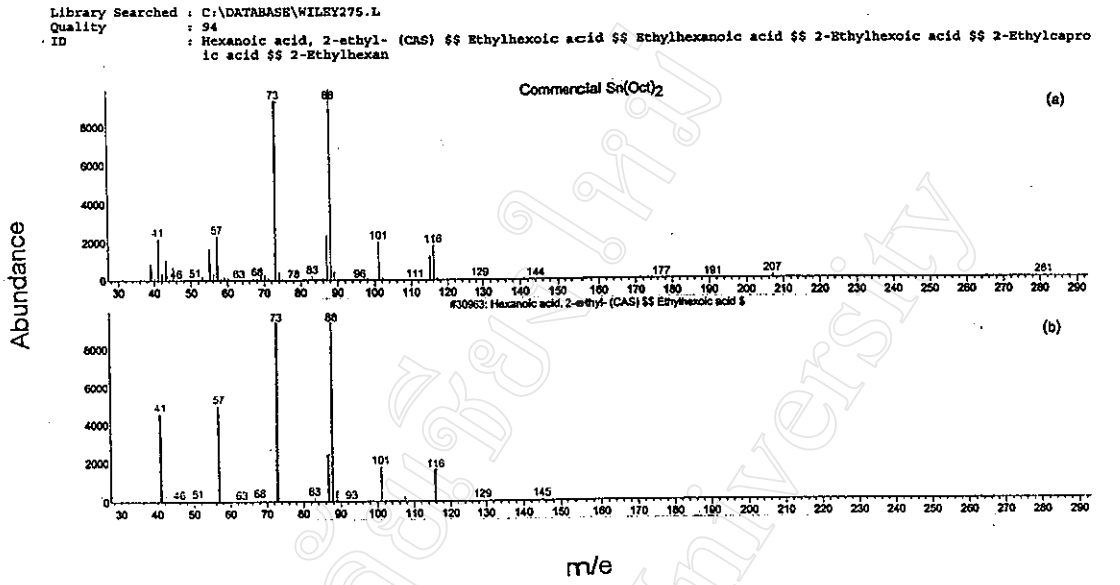

Figure 3.15 Comparison of the MS spectrum of (a) the commercial $Sn(Oct)_2$ peak at 3.97 min (in Figure 3.13) with (b) a reference spectrum of 2-ethyl hexanoic acid.

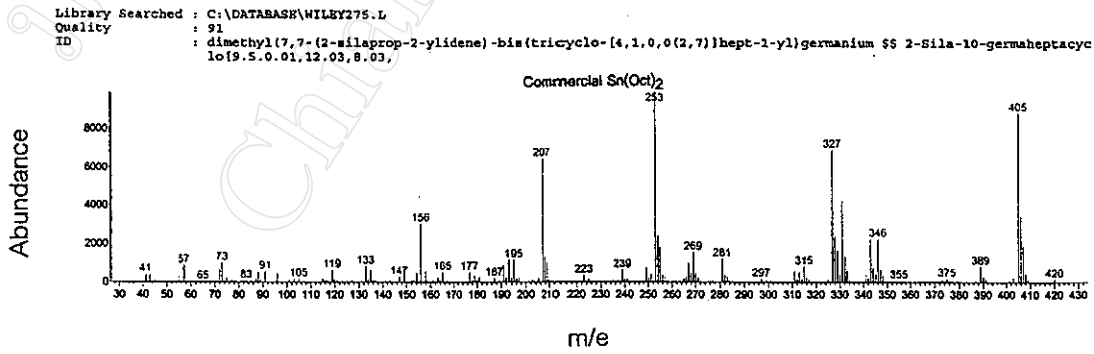

Figure 3.16 MS spectrum of the commercial $Sn(Oct)_2$ peak at 8.12 min (in Figure 3.13) showing the top mass (m/e) peak of 405 corresponding to $Sn(Oct)_2$.

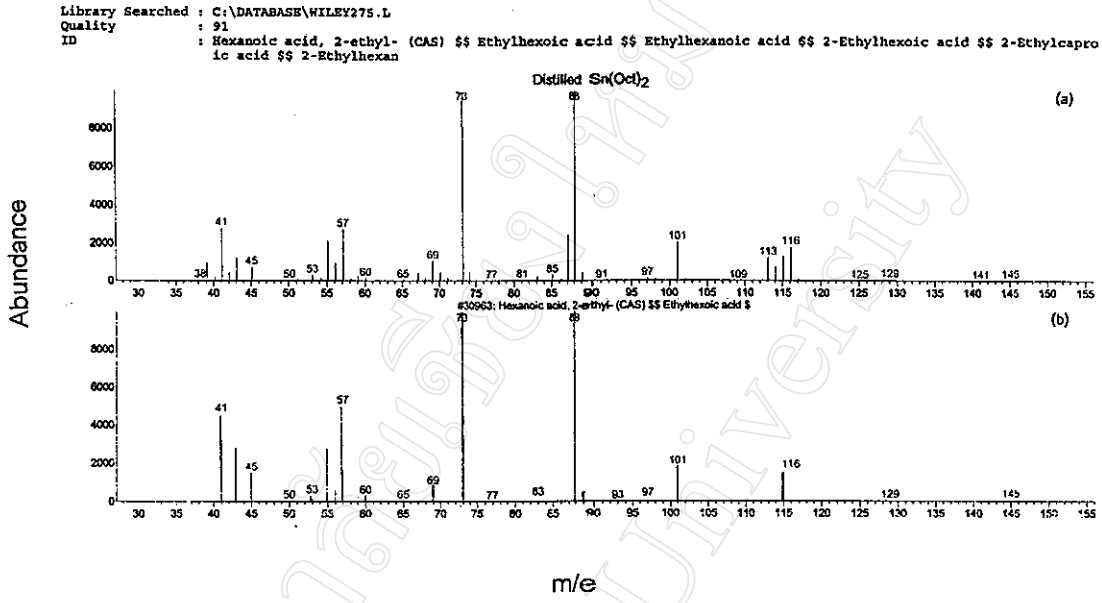

Figure 3.17 Comparison of the MS spectrum of (a) the distilled $Sn(Oct)_2$ peak at 4.36 min (in Figure 3.14) with (b) a reference spectrum of 2-ethyl hexanoic acid.

3.4.2 Stannous Oxalate

The commercial stannous oxalate, SnOx, used in this project as an alternative catalyst to $Sn(Oct)_2$ was a finely divided white powder. Unlike $Sn(Oct)_2$, it is not so hygroscopic and was used without further purification.

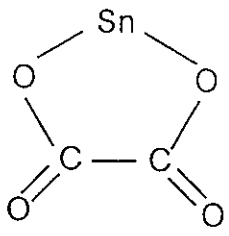

stannous oxalate

SnOx

3.4.3 Diethylene Glycol

Diethylene glycol, used as an initiator in conjunction with either $Sn(Oct)_2$ or SnOx as catalyst, was purified by vacuum distillation (Figure 3.18). Due to its hygroscopic nature, the main impurity in diethylene glycol is usually moisture. The constant boiling fraction at 110 °C / 3-4 mm Hg pressure was collected. (cf. diethylene glycol lit. [29] b. pt. = 133 °C / 14 mm Hg). Purified diethylene glycol was obtained as a clear colourless liquid and was stored over molecular sieves 4 Å until required for use. Its IR spectra both before and after purification are compared in Figures 3.19 and 3.20.

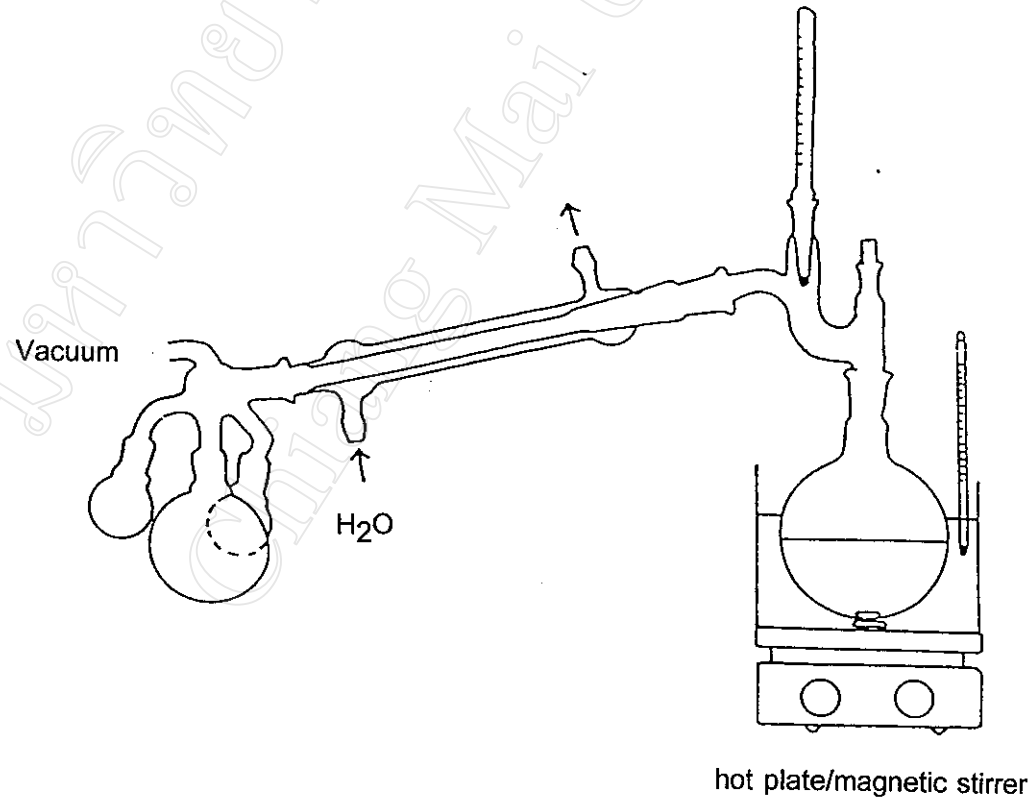

Figure 3.18 Vacuum distillation apparatus used for diethylene glycol purification.

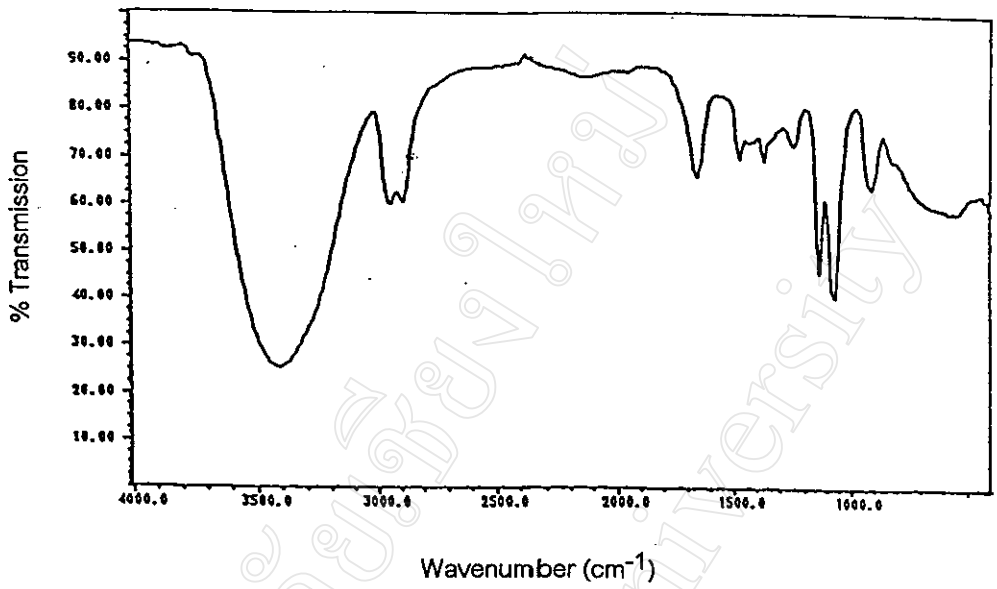

Figure 3.19 IR spectrum of diethylene glycol before vacuum distillation.

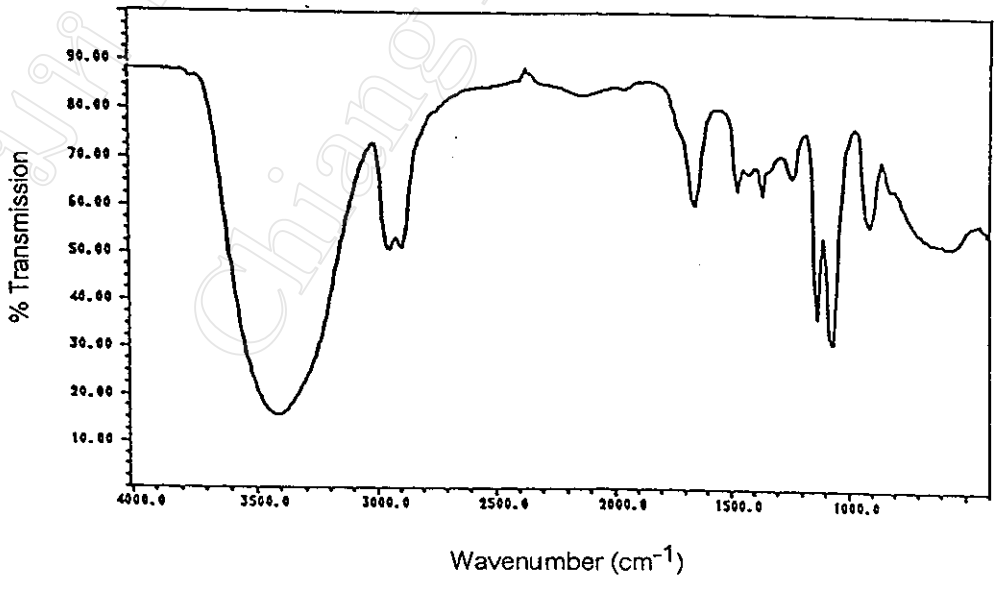

Figure 3.20 IR spectrum of diethylene glycol after vacuum distillation.

Table 3.7 Main vibrational assignments in the IR spectra of the diethylene glycol both before and after vacuum distillation.

$$HO-CH_2-CH_2-O-CH_2-CH_2-OH$$

diethylene glycol

VIBRATIONAL ASSIGNMENT	WAVENUMBER (cm^{-1})	
	Before vacuum distillation	After vacuum distillation
O – H stretching	3700 - 3000	3700 – 3000
C – H stretching	2975 - 2900	2975 – 2900
C – H bending	1460, 1360	1460, 1360
C – O – C stretching	1150 - 1050	1150 – 1050